AIAA JOURNAL
Vol. 45, No. 9, September 2007

Minimum-State Unsteady Aerodynamic Shape Sensitivities Using Sensitivity of Optimal Solutions to Problem Parameters

Marat Mor* and Eli Livne†
University of Washington, Seattle, Washington 98195-2400

DOI: 10.2514/1.24480

A mathematical-programming-based technique for fitting minimum-state rational approximations to unsteady aerodynamic generalized force matrices was presented recently. It allows for simultaneous determination of all series parameters involved, including the aerodynamic lag roots. Its solution is unique, and convergence of the solution process, based on standard mathematical programming techniques, allows accurate determination of all unknown variables. An improvement of the math-programming minimum-state fitting is presented here, and it is developed further to include sensitivity analysis for the resulting minimum-state series, free of the nonuniqueness and convergence issues that plagued previous attempts to obtain sensitivities of minimum-state fits. A variable planform double-swept forward wing case is used to demonstrate performance of the fitting technique itself, shape sensitivity calculations, and Taylor-series-based approximations that can be used to replace detailed full-order analysis in the course of multidisciplinary design optimization of flight vehicles.

Nomenclature

$[A_0]$, $[A_1]$, $[A_2]$	=	minimum-state approximation matrices corresponding to aerodynamic stiffness, damping, and inertia, respectively
$a^{(0)}$, $a^{(1)}$, $a^{(2)}$	=	elements of the matrices $[A_0]$, $[A_1]$, $[A_2]$
b	=	reference semichord length of wing
$[C]$	=	structural viscous damping matrix
c	=	reference chord length of wing
$[D]$, $[E]$	=	minimum-state approximation matrices representing lag terms
d, e	=	elements of the matrices $[D]$, $[E]$
DV	=	design variable
E	=	Young's modulus
f	=	objective function (least-squares error, to be minimized)
G	=	shear modulus
$[H]$	=	Hessian matrix
$[I]$	=	identity matrix
Im	=	imaginary part
j	=	pure imaginary number, $j = -\sqrt{1}$
$[K]$	=	stiffness matrix
k	=	reduced frequency
L	=	half-span length of wing
$[M]$	=	mass matrix
$[N]$	=	first-order derivative matrix of active constraints
n	=	number of structural degrees of freedom
$\bar{n}$	=	rank of Hessian matrix
n_a	=	number of active constraints
n_k	=	number of reduced frequencies
n_{lag}	=	number of lag terms
$[Q]$	=	aerodynamic generalized force coefficients matrix
$[\bar{Q}]$	=	approximated aerodynamic generalized force coefficients matrix
q	=	elements of the matrix $[Q]$
$\bar{q}$	=	elements of the matrix $[\bar{Q}]$
q_D	=	dynamic pressure
$[R]$	=	diagonal matrix of aerodynamic lag roots
Re	=	real part
{RHS}	=	right-hand side vector
t	=	thickness of double-swept forward test wing
V	=	speed of flight
X, Y	=	elements of the solution vector $\{x^*\}$
$\{x^*\}$	=	optimal solution vector
$[Z]$	=	second-order derivative matrix of active constraints
γ	=	roots of lag terms
Δ	=	difference between exact and approximated solution [see Eq. (9)]
Λ	=	inboard sweep angle of wing
$\{\xi\}$	=	vector of generalized structural dynamic motions
ρ	=	air density
ω	=	frequency of oscillation

Subscripts and Superscripts

0	=	original, design point
max	=	maximum
new	=	new, changed configuration point
REF	=	reference point

Presented as Paper 2158 at the 47th AIAA/ASME/ASCE/AHS/ASC Structures, Structural Dynamics, and Materials Conference, Newport, RI, 1–4 May 2006; received 6 April 2006; revision received 22 January 2007; accepted for publication 23 January 2007.

*Postdoctoral Research Fellow, Department of Aeronautics and Astronautics; mor@aa.washington.edu. Member AIAA.

†Professor, Department of Aeronautics and Astronautics; eli@aa.washington.edu. Associate Fellow AIAA.

I. Introduction

THE minimum-state approximation (MIST) is widely used in aeroservoelasticity to convert unsteady aerodynamic models from the frequency to the time domain [1–5]. The method involves fitting a rational function approximation to tabulated frequency-dependent aerodynamic matrices, and it was originally based on an iterative double least-squares fitting process. The iterative nature of the process made it time-consuming, and, although acceptable approximants could be obtained without complete convergence of the iterations, that presented a challenge regarding the computation of *sensitivities* of the resulting models with respect to planform shape

variations. A method for obtaining planform shape sensitivities of MIST approximants was presented in [6,7]. Recently a method for obtaining MIST approximants had been presented [8]. The method replaces the double least-squares process with a gradient-based nonlinear programming (NLP) approach in which the matrices and lag roots of the MIST approximant are determined as the solution of a math-programming problem. With the new unique optimal MIST approximants, it has become possible to use techniques for obtaining sensitivities of optimal solutions to problem parameters to calculate sensitivities of the MIST approximants to planform shapes. In the following sections we will extend the new NLP/MIST method to include planform shape sensitivities free of the iteration, convergence, and uniqueness issues of previous formulations. The development of design-oriented state-space aeroservoelastic models with analytic shape sensitivities is a necessary step on the road to integrated multidisciplinary design optimization of flight vehicles allowing for planform shape variations.

II. Formulation

The linear aeroelastic problem can be formulated in the frequency domain as follows [1–8]:

$$(-\omega^2[M] + j\omega[C] + [K] - q_D[Q(j\omega)])\{\boldsymbol{\xi}(j\omega)\} = 0 \tag{1}$$

where $[Q(j\omega)]$ is the Fourier-transformed aerodynamic generalized force coefficients matrix, the matrices $[M]$, $[C]$, $[K]$ are generalized mass, damping, and stiffness matrices, respectively, q_D is dynamic pressure, and ω is the oscillation frequency. The vector of generalized structural dynamic motions using some modal base is $\{\boldsymbol{\xi}(j\omega)\}$. Equation (1) represents free unexcited motion.

To create a linear-time-invariant (LTI) state-space model of the system, an approximation of the $[Q]$ matrix in the form of a rational function minimum state is introduced:

$$[Q(jk)] \approx [\bar{Q}(jk)] = [A_0] + jk[A_1] + (jk)^2[A_2] + jk[D](jk[I] + [R])^{-1}[E] \tag{2}$$

where $[\bar{Q}(jk)]$ is the approximated aerodynamic generalized force coefficients matrix, and k is the reduced frequency of oscillation

$$k = \frac{\omega b}{V} \tag{3}$$

It depends on the oscillation frequency ω, the reference semichord length b, and the speed of flight V. Constant real matrices include $[A_0]$, $[A_1]$, $[A_2]$, $[D]$, $[E]$, $[R]$, where $[R]$ is a positive diagonal matrix containing the roots of the aerodynamic lag terms γ:

$$[R] = \begin{bmatrix} \gamma_1 & 0 & .. & 0 \\ 0 & \gamma_2 & .. & 0 \\ : & : & :: & 0 \\ 0 & 0 & .. & \gamma_{n_{\text{lag}}} \end{bmatrix} \tag{4}$$

In Eq. (4), n_{lag} is a number of the aerodynamic lag roots.

The approximated generalized aerodynamic matrix (without gust excitation and control modes columns for simplicity but without the loss of generality) is a square matrix of the order $n \times n$, where n is the number of structural degrees of freedom used:

$$[\bar{Q}(jk)]_{n\times n} = \begin{bmatrix} \bar{q}_{11} & \bar{q}_{12} & . & \bar{q}_{1n} \\ \bar{q}_{21} & \bar{q}_{22} & . & \bar{q}_{2n} \\ . & . & . & . \\ \bar{q}_{n1} & \bar{q}_{n2} & . & \bar{q}_{nn} \end{bmatrix} \tag{5}$$

Similarly, the elements of the matrix $[Q(jk)]$ will be denoted $q_{lm}(jk)$. Expanding Eq. (2) one can write a general expression for the elements of an approximated (fitted) matrix $[\bar{Q}(jk)]$ as follows:

$$\begin{aligned} \bar{q}_{lm}(jk) - a_{lm}^{(0)} &= jka_{lm}^{(1)} + (jk)^2 a_{lm}^{(2)} + \sum_{i=1}^{n_{\text{lag}}} \frac{jk}{jk+\gamma_i} d_{li}e_{im} \\ &= k^2\left(-a_{lm}^{(2)} + \sum_{i=1}^{n_{\text{lag}}} \frac{1}{k^2+\gamma_i^2} d_{li}e_{im}\right) \\ &\quad + jk\left(a_{lm}^{(1)} + \sum_{i=1}^{n_{\text{lag}}} \frac{\gamma_i}{k^2+\gamma_i^2} d_{li}e_{im}\right) \end{aligned} \tag{6}$$

The matrix $[A_0]$ is set to be equal to the tabulated steady $[Q(jk=0)]$. The solution for the matrices $[A_1]$, $[A_2]$, $[D]$, $[E]$ for the classical MIST method, where the aerodynamic lag roots [Eq. (4)] are predetermined by the user, involves an iterative nonlinear double least-squares fitting process. The nonlinearity of the $[D]$ $(jk[I] + [R])^{-1}$ $[E]$ term is handled by guessing $[D]$, fixing it, and solving for $[E]$, then fixing $[E]$ and solving for $[D]$, etc., [1–5]. The goal is to minimize the sum of the squares of the differences between all tabulated terms $q_{lm}(jk)$ and fitted terms $\bar{q}_{lm}(jk)$ [based on Eq. (2)] over all reduced frequencies at which aerodynamic matrices are given: the tabulated reduced frequencies. As discussed in the previous work [6,7], due to the nonlinear nature of the problem, the $[D]-[E]-[D]$ procedure has convergence issues. Many iterations are required for convergence of the $[D]$ and $[E]$ matrices. It is found that well before convergence of the $[D]$ and $[E]$ matrices is achieved, the overall error of the approximant [Eq. (2)] can be reduced to within acceptable bounds, and, thus, the iterative process can be stopped. This creates a problem, however, when it comes to sensitivity analysis, which has to be carried out at a converged solution point.

III. MIST Approximants by Math-Programming-Based Fitting

Adding the lag terms matrix $[R]$ to the list of unknowns in the curve fitting problem adds to the complexity and the nonlinearity of the problem. This was addressed by Nissim [8,9] who used a gradient-based math-programming procedure to obtain the solution. In his method, Nissim used the $[D]$, $[E]$, $[R]$ matrices as unknowns of the least-squares math-programming problem, with the $[A_1]$, $[A_2]$ linked to $[D]$, $[E]$, $[R]$ and calculated based on an explicit least-squares problem formulation.[‡] This serves to reduce the number of unknowns in the math-programming problem from those associated with $[A_1]$, $[A_2]$, $[D]$, $[E]$, $[R]$ to those associated with $[D]$, $[E]$, $[R]$ only. In the following, Nissim's method is modified as follows:

In a first step, the goal is to obtain MIST approximant matrices that will be used as an initial guess (precondition) in the math-programming process. An initial matrix $[D]$ and a diagonal matrix $[R]$ are picked, and a few $[D]-[E]-[D]$ double least-squares iterations are carried out. Based on [6], usually 10–20 iterations are enough to drastically reduce the initial least-squares method (LSM) error. In this process, the lag terms in the matrix $[R]$ remain constant at their initial guess values. The LSM error f, which is also the objective function for the optimization problem presented here, is given by

$$\begin{aligned} f &= \sum_{v=1}^{n_k} \sum |[\bar{Q}(jk_v)] - [Q(jk_v)]|^2 \\ &= \sum_{v=1}^{n_k} \sum_{l=1}^{n} \sum_{m=1}^{n} \{[\Delta_{lm}^{\text{Re}}(k_v)]^2 + [\Delta_{lm}^{\text{Im}}(k_v)]^2\} \end{aligned} \tag{7}$$

and should be minimized with the following constraints to ensure stability of the resulting linear-time-invariant state-space model of the unsteady aerodynamics:

$$\gamma_i > 0, \qquad i = 1, \ldots, n_{\text{lag}} \tag{8}$$

[‡]In this problem the matrices $[A_1]$ and $[A_2]$ are explicitly obtained through the rest of the terms (matrices $[D]$, $[E]$, $[R]$) in the imaginary and real parts of Eq. (2), respectively.

In Eq. (7), the symbol $\sum$ denotes the sum over all members of the matrix, and the errors in real and imaginary parts of the approximation at tabulated reduced frequencies are

$$\begin{aligned}\Delta^{\mathrm{Re}}_{lm}(k) &= \mathrm{Re}[\bar{q}_{lm}(jk) - q_{lm}(jk)] \\ &= k^2\left(\sum_{i=1}^{n_{\mathrm{lag}}} \frac{1}{k^2+\gamma_i^2} d_{li}e_{im} - a^{(2)}_{lm}\right) - \mathrm{Re}[q_{lm}(jk) - q_{lm}(0)] \\ \Delta^{\mathrm{Im}}_{lm}(k) &= \mathrm{Im}[\bar{q}_{lm}(jk) - q_{lm}(jk)] \\ &= k\left(a^{(1)}_{lm} + \sum_{i=1}^{n_{\mathrm{lag}}} \frac{\gamma_i}{k^2+\gamma_i^2} d_{li}e_{im}\right) - \mathrm{Im}[q_{lm}(jk)] \end{aligned} \tag{9}$$

It is important to note that the constraints in Eq. (8) are actually inactive, because experience shows [8] that the math-programming solution settles at lag roots that are stable. In fact, if one of the lag-root constraints, hypothetically, would become active, then the corresponding $[D]$ $[E]$ matrix would be a part of $[A_0]$ matrix, with resulting numerical consequences due to the nonuniqueness of the corresponding $[D]$ $[E]$ and $[A_0]$ solutions in this case.

The math-programming optimization procedure can now start, with elements of the matrices $[D]_{n\times n_{\mathrm{lag}}}$ and $[R]_{n_{\mathrm{lag}}\times n_{\mathrm{lag}}}$ being the unknowns. Note, that because the direct multiplication of the matrices $[D]$ and $[E]$ is involved, there is an infinite number of possible $[D]$ and $[E]$ with the same product $[D]$ $[E]$, and the solution is not unique. To obtain a unique solution [9] the matrix $[D]$ is normalized so that the first row is constant and is a unit row vector. Therefore, only $(n-1)n_{\mathrm{lag}}$ number of design variables is associated with the matrix $[D]$ in the math-programming process. Together with the n_{lag} unknowns of the diagonal $[R]$ matrix, the math-programming process involves nn_{lag} unknowns. The total number of MIST unknowns is $2nn_{\mathrm{lag}}$ for the $[D]$, $[E]$, $[R]$ matrices and $2n^2$ for $[A_1]$ and $[A_2]$.

Throughout the math-programming solution process the $[A_1]$, $[A_2]$, $[E]$ matrices are determined explicitly from the $[D]$, $[R]$ matrices using the least-squares solution:

$$\begin{bmatrix} A_1 \\ A_2 \\ E \end{bmatrix} \approx ([S]^T[S])^{-1}[S]^T \begin{bmatrix} \mathrm{Re}[Q(k_1)] - [A_0] \\ \mathrm{Im}[Q(k_1)] \\ \mathrm{Re}[Q(k_2)] - [A_0] \\ \mathrm{Im}[Q(k_2)] \\ \cdots \\ \mathrm{Re}[Q(k_{n_k})] - [A_0] \\ \mathrm{Im}[Q(k_{n_k})] \end{bmatrix} \tag{10}$$

where

$$[S] = \begin{bmatrix} [0] & -k_1^2[I] & [D][\Pi_R(k_1)] \\ k_1[I] & [0] & [D][\Pi_I(k_1)] \\ [0] & -k_2^2[I] & [D][\Pi_R(k_2)] \\ k_2[I] & [0] & [D][\Pi_I(k_2)] \\ \cdots & \cdots & \cdots \\ [0] & -k_{n_k}^2[I] & [D][\Pi_R(k_{n_k})] \\ k_{n_k}[I] & [0] & [D][\Pi_I(k_{n_k})] \end{bmatrix} \tag{11}$$

and

$$\begin{aligned}[\Pi_R(k)] &= \begin{bmatrix} \frac{k^2}{k^2+\gamma_1^2} & 0 & 0 \\ 0 & \frac{k^2}{k^2+\gamma_2^2} & 0 \\ 0 & 0 & \ddots \end{bmatrix}, \\ [\Pi_I(k)] &= \begin{bmatrix} \frac{k\gamma_1}{k^2+\gamma_1^2} & 0 & 0 \\ 0 & \frac{k\gamma_2}{k^2+\gamma_2^2} & 0 \\ 0 & 0 & \ddots \end{bmatrix} \end{aligned} \tag{12}$$

It is important to note that the same objective function is used for the math-programming process and the explicit least-squares solution. The result is a solution for all elements $[A_1]$, $[A_2]$, $[D]$, $[E]$, $[R]$ of the MIST approximant that is identical to what would be obtained if the math-programming process would involve Eq. (7) as objective and all $[A_1]$, $[A_2]$, $[D]$, $[E]$, $[R]$ elements as unknowns. Any gradient-based math-programming procedure can be used for the math-programming part of the procedure just outlined.

IV. Sensitivity of Optimum Solution to Problem Parameters

Assuming that a MIST approximant had been obtained as a converged solution of a constrained gradient-based math-programming problem, the sensitivity of the optimum solution to a problem parameter DV is obtained by differentiating the Kuhn–Tucker optimality conditions [10]. Such a problem parameter in our case can be any geometric variable used to define the planform of a configuration for which unsteady aerodynamic loads are calculated. The MIST approximation is determined by the math-programming process described in the preceding section for a given planform. The question now is how this MIST approximation and its associated state-space model will vary with variation of the shape of the configuration. If $\{\boldsymbol{x}^*\}$ is the solution to the problem $\min f(\{x\})$ subject to a set of constraints, then

$$\begin{aligned}&([H]_{\bar{n}\times\bar{n}} - [Z]_{\bar{n}\times\bar{n}})\frac{d\{\boldsymbol{x}^*\}_{\bar{n}}}{dDV} - [N]_{\bar{n}\times n_a}\frac{d\{\lambda\}_{n_a}}{dDV} + \frac{\partial\{\nabla f\}_{\bar{n}}}{\partial DV} \\ &\quad - \frac{\partial[N]_{\bar{n}\times n_a}}{\partial DV}\{\lambda\}_{n_a} = \{0\}_{\bar{n}} \\ &[N]^T_{n_a\times\bar{n}}\frac{d\{\boldsymbol{x}^*\}_{\bar{n}}}{dDV} + \frac{\partial\{\gamma_a\}_{n_a}}{\partial DV} = \{0\}_{n_a}\end{aligned} \tag{13}$$

Here $[H]_{\bar{n}\times\bar{n}}$ is the Hessian matrix of the objective function f (calculated at the design point where the optimal solution is obtained). Because there are no active constraints, $n_a = 0$ in our case, the vector of the Lagrange multipliers $\{\lambda\}_{n_a}$ and the active constraints' first- and second-order derivatives matrices $[N]_{\bar{n}\times n_a}$ and $[Z]_{\bar{n}\times\bar{n}}$ are zero. The problem, thus, simplifies to

$$[H]_{\bar{n}\times\bar{n}}\frac{d\{\boldsymbol{x}^*\}_{\bar{n}}}{dDV} + \frac{\partial\{\nabla f\}_{\bar{n}}}{\partial DV} = \{0\}_{\bar{n}} \tag{14}$$

where $\{\boldsymbol{x}^*\}_{\bar{n}}$ is the solution vector which includes all the variables of the matrices $[A_1]$, $[A_2]$, $[D]$, $[E]$, $[R]$, except of the first row of the $[D]$ matrix which is kept constant (and therefore its derivative is a zero vector $[0]_{1\times n_{\mathrm{lag}}}$)

$$\begin{aligned}&\{\boldsymbol{x}^*\}^T_{\bar{n}} \\ &= \begin{bmatrix} a^{(1)}_{11}\ldots a^{(1)}_{nn} & a^{(2)}_{11}\ldots a^{(2)}_{nn} & d_{21}\ldots d_{nn_{lag}} & e_{11}\ldots e_{n_{\mathrm{lag}}n} & \gamma_1\ldots\gamma_{n_{\mathrm{lag}}} \end{bmatrix}\end{aligned} \tag{15}$$

The number of MIST unknowns is

$$\bar{n} = 2n^2 + 2n\cdot n_{\mathrm{lag}} \tag{16}$$

We can now proceed to obtain analytical expressions for elements of the Hessian matrix as well as the derivative of the objective function's gradient with respect to the problem parameter (configuration shape design variable) $\partial\{\nabla f\}_{\bar{n}}/\partial DV$. By differentiating Eq. (7) the first- and the second-order derivatives of the objective function can be obtained as follows:

$$\frac{\partial f}{\partial X} = 2\sum_{v=1}^{n_k}\sum_{l=1}^{n}\sum_{m=1}^{n}\left(\Delta^{\mathrm{Re}}_{lm}(k_v)\frac{\partial\Delta^{\mathrm{Re}}_{lm}(k_v)}{\partial X} + \Delta^{\mathrm{Im}}_{lm}(k_v)\frac{\partial\Delta^{\mathrm{Im}}_{lm}(k_v)}{\partial X}\right) \tag{17}$$

and

$$\begin{aligned}\frac{\partial^2 f}{\partial X\partial Y} = 2\sum_{v=1}^{n_k}\sum_{l=1}^{n}\sum_{m=1}^{n}\Bigg(&\Delta^{\mathrm{Re}}_{lm}(k_v)\frac{\partial^2\Delta^{\mathrm{Re}}_{lm}(k_v)}{\partial X\partial Y} + \frac{\partial\Delta^{\mathrm{Re}}_{lm}(k_v)}{\partial X}\frac{\partial\Delta^{\mathrm{Re}}_{lm}(k_v)}{\partial Y} \\ &+ \Delta^{\mathrm{Im}}_{lm}(k_v)\frac{\partial^2\Delta^{\mathrm{Im}}_{lm}(k_v)}{\partial X\partial Y} + \frac{\partial\Delta^{\mathrm{Im}}_{lm}(k_v)}{\partial X}\frac{\partial\Delta^{\mathrm{Im}}_{lm}(k_v)}{\partial Y}\Bigg)\end{aligned} \tag{18}$$

Here the variables X and Y represent the members of the solution vector $\{\boldsymbol{x}^*\}$ [Eq. (15)]. The first-order derivatives in Eqs. (17) and (18) are listed below:

$$\frac{\partial \Delta_{lm}^{\mathrm{Re}}}{\partial a_{rs}^{(1)}} = 0 \qquad \frac{\partial \Delta_{lm}^{\mathrm{Im}}}{\partial a_{rs}^{(1)}} = \begin{cases} k, & r = l, s = m \\ 0, & \text{else} \end{cases} \tag{19}$$

$$\frac{\partial \Delta_{lm}^{\mathrm{Re}}}{\partial a_{rs}^{(2)}} = \begin{cases} -k^2 & r = l, s = m \\ 0, & \text{else} \end{cases} \qquad \frac{\partial \Delta_{lm}^{\mathrm{Im}}}{\partial a_{rs}^{(2)}} = 0 \tag{20}$$

$$\begin{aligned} \frac{\partial \Delta_{lm}^{\mathrm{Re}}}{\partial d_{\bar{r}p}} &= \begin{cases} \frac{k^2}{k^2+\gamma_p^2} e_{pm}, & \bar{r} = l, \forall\ m, p \\ 0, & \text{else} \end{cases} \\ \frac{\partial \Delta_{lm}^{\mathrm{Im}}}{\partial d_{\bar{r}p}} &= \begin{cases} \frac{k\gamma_p}{k^2+\gamma_p^2} e_{pm}, & \bar{r} = l, \forall\ m, p \\ 0, & \text{else} \end{cases} \end{aligned} \tag{21}$$

$$\begin{aligned} \frac{\partial \Delta_{lm}^{\mathrm{Re}}}{\partial e_{ps}} &= \begin{cases} \frac{k^2}{k^2+\gamma_p^2} d_{lp}, & s = m, \forall\ l, p \\ 0, & \text{else} \end{cases} \\ \frac{\partial \Delta_{lm}^{\mathrm{Im}}}{\partial e_{ps}} &= \begin{cases} \frac{k\gamma_p}{k^2+\gamma_p^2} d_{lp}, & s = m, \forall\ l, p \\ 0, & \text{else} \end{cases} \end{aligned} \tag{22}$$

$$\frac{\partial \Delta_{lm}^{\mathrm{Re}}}{\partial \gamma_p} = -2\frac{k^2\gamma_p}{(k^2+\gamma_p^2)^2} d_{lp} e_{pm} \qquad \frac{\partial \Delta_{lm}^{\mathrm{Im}}}{\partial \gamma_p} = k\frac{k^2-\gamma_p^2}{(k^2+\gamma_p^2)^2} d_{lp} e_{pm} \tag{23}$$

In Eqs. (19–23) the indices vary as follows:

$$l, m, r, s = 1, 2, \ldots, n \quad \text{and} \quad \bar{r} = 2, 3, \ldots, n \tag{24}$$

and

$$p = 1, 2, \ldots, n_{\mathrm{lag}} \tag{25}$$

For the second-order derivatives, the following expressions are obtained:

$$\frac{\partial^2 \Delta_{lm}^{\mathrm{Re}}}{\partial a_{r_1 s_1}^{(1)} \partial X} = \frac{\partial^2 \Delta_{lm}^{\mathrm{Im}}}{\partial a_{r_1 s_1}^{(1)} \partial X} = \frac{\partial^2 \Delta_{lm}^{\mathrm{Re}}}{\partial a_{r_1 s_1}^{(2)} \partial X} = \frac{\partial^2 \Delta_{lm}^{\mathrm{Im}}}{\partial a_{r_1 s_1}^{(2)} \partial X} = 0, \quad \forall\ X \in \{\boldsymbol{x}^*\} \tag{26}$$

$$\begin{aligned} \frac{\partial^2 \Delta_{lm}^{\mathrm{Re}}}{\partial d_{\bar{r}_1 p_1} \partial e_{p_2 s_2}} &= \begin{cases} \frac{k^2}{k^2+\gamma_{p_1}^2}, & \bar{r}_1 = l, s_2 = m, p_1 = p_2 \\ 0, & \text{else} \end{cases} \\ \frac{\partial^2 \Delta_{lm}^{\mathrm{Im}}}{\partial d_{\bar{r}_1 p_1} \partial e_{p_2 s_2}} &= \begin{cases} \frac{k\gamma_{p_1}}{k^2+\gamma_{p_1}^2}, & \bar{r}_1 = l, s_2 = m, p_1 = p_2 \\ 0, & \text{else} \end{cases} \end{aligned} \tag{27}$$

$$\begin{aligned} \frac{\partial^2 \Delta_{lm}^{\mathrm{Re}}}{\partial d_{\bar{r}_1 p_1} \partial \gamma_{p2}} &= \begin{cases} -2\frac{k^2\gamma_{p_1}}{(k^2+\gamma_{p_1}^2)^2} e_{p_1 m}, & \bar{r}_1 = l, p_1 = p_2, \forall\ m \\ 0, & \text{else} \end{cases} \\ \frac{\partial^2 \Delta_{lm}^{\mathrm{Im}}}{\partial d_{\bar{r}_1 p_1} \partial \gamma_{p_2}} &= \begin{cases} k\frac{k^2-\gamma_{p_1}^2}{(k^2+\gamma_{p_1}^2)^2} e_{p_1 m}, & \bar{r}_1 = l, p_1 = p_2, \forall\ m \\ 0, & \text{else} \end{cases} \end{aligned} \tag{28}$$

$$\begin{aligned} \frac{\partial^2 \Delta_{lm}^{\mathrm{Re}}}{\partial e_{p_1 s_1} \partial \gamma_{p_2}} &= \begin{cases} -2\frac{k^2\gamma_{p_2}}{(k^2+\gamma_{p_1}^2)^2} d_{lp_1}, & s_1 = m, p_1 = p_2, \forall\ l \\ 0, & \text{else} \end{cases} \\ \frac{\partial^2 \Delta_{lm}^{\mathrm{Im}}}{\partial e_{p_1 s_1} \partial \gamma_{p_2}} &= \begin{cases} k\frac{k^2-\gamma_{p_1}^2}{(k^2+\gamma_{p_1}^2)^2} d_{lp_1}, & s_1 = m, p_1 = p_2, \forall\ l \\ 0, & \text{else} \end{cases} \end{aligned} \tag{29}$$

$$\begin{aligned} \frac{\partial^2 \Delta_{lm}^{\mathrm{Re}}}{\partial \gamma_{p_1} \partial \gamma_{p_2}} &= 2k^2 \frac{3\gamma_{p_1}^2 - k^2}{(k^2+\gamma_{p_1}^2)^3} d_{lp_1} e_{p_1 m}, \qquad p_1 = p_2 \\ \frac{\partial^2 \Delta_{lm}^{\mathrm{Im}}}{\partial \gamma_{p_1} \partial \gamma_{p_2}} &= 2k\gamma_{p_1} \frac{\gamma_{p_1}^2 - 3k^2}{(k^2+\gamma_{p_1}^2)^3} d_{lp_1} e_{p_1 m}, \qquad p_1 = p_2 \end{aligned} \tag{30}$$

Here, the indices l, m, r, $\bar{r}$, s, and p vary according to Eqs. (24) and (25). The values $\Delta_{lm}^{\mathrm{Re}}$ and $\Delta_{lm}^{\mathrm{Im}}$ are calculated in Eqs. (9) (for the optimal solution).

Appendix A lists all elements of the Hessian matrix, which are derived by substituting Eqs. (19–30) into Eqs. (17) and (18). The derivatives of the gradient of the objective function with respect to the problem parameters (planform shape design variables) form the right-hand side of Eq. (31) [see Eq. (14)], which depends on the derivatives of the aerodynamic influence coefficients matrix $\partial[Q(jk)]/\partial DV$. The following linear set of equations is obtained:

$$[H(\boldsymbol{x}^*)]_{\bar{n}\times\bar{n}} \frac{d\{\boldsymbol{x}^*\}_{\bar{n}}}{dDV} = \left\{ \mathrm{RHS}\left(\boldsymbol{x}^*, \frac{\partial q(jk)}{\partial DV} \right) \right\}_{\bar{n}} \tag{31}$$

where the terms $\partial q(jk)/\partial DV$ are evaluated numerically using finite differences or analytically [10–15], and RHS stands for right-hand side of Eq. (31): $(\{\mathrm{RHS}\} = -\partial\{\nabla f\}/\partial DV$, see Appendix B).

Building on Nissim's work [8,9], we have now obtained a modified MIST fitting procedure which allows all elements of the MIST series, including lag terms, to be determined effectively and uniquely, and which includes calculation of analytic sensitivities of the MIST approximation with respect to planform design variables of the configurations analyzed. Once analytic sensitivities of the MIST approximants with respect to planform shape variables are available, Taylor series approximations can be used in an approximations concepts/nonlinear programming strategy (NLP/AC) to design optimization of flight vehicles whose shape varies during the design process [10,16]. For example, a direct Taylor series approximation will be of the form

$$\{\boldsymbol{x}_{\mathrm{new}}^*\}_{\bar{n}} = \{\boldsymbol{x}_0^*\}_{\bar{n}} + \frac{d\{\boldsymbol{x}^*\}_{\bar{n}}}{dDV}(DV_{\mathrm{new}} - DV_0) \tag{32}$$

Here the indices 0 and "new" indicate the solutions for the initial and changed shapes. Approximations of this type for all elements of the $[A_1]$, $[A_2]$, $[D]$, $[E]$, $[R]$ matrices make it possible for the multidisciplinary design optimization process to effectively calculate variations of the state-space models involved as a result of shape variations without the need to carry out full aerodynamic analysis as well as full MIST fitting for every change in planform shape. This is key to the practicality of any flight vehicle multidisciplinary design optimization (MDO) strategy.

V. Double-Swept Forward Wing Example

The double-swept forward wing (M-W wing, see [6,17]) was chosen to examine the results of MIST analysis and its optimal solution sensitivity in the case of major planform changes. The geometry of the wing is shown in Fig. 1. The chord length is $c = 76$ mm and the half-span length is $L = 305$ mm. The sweep angle of the inboard wing Λ is varied from -30 to 30 deg. The wing is assumed to have a thickness $t = 1$ mm and its structural material characteristics are $E = 73.8$ GPa, $G = 27.6$ GPa, $\rho = 2768$ Kg/m^3.

The structural finite element results for the wing for the different values of the inboard sweep angle Λ were calculated using MSC NASTRAN [18]. The first ten modes were used for the aeroelastic analysis using Mach $= 0$ aerodynamics produced by the unsteady aerodynamic ZAERO panel code [19].

Assuming a constant matrix $[R]$, the classical $[D]-[E]-[D]$ iteration process was launched. As mentioned in [6] this process has convergence problems especially in complex cases and it is rarely possible to obtain full convergence. However, even 20 iterations provide a good start for the math-programming process. Figure 2

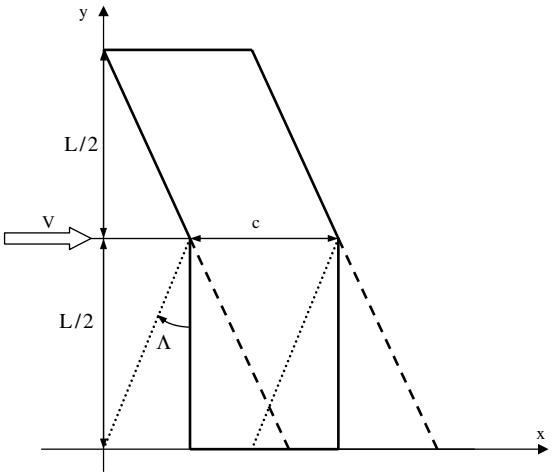

Fig. 1 M-W wing [6,17], planform shape variations of the inner wing.

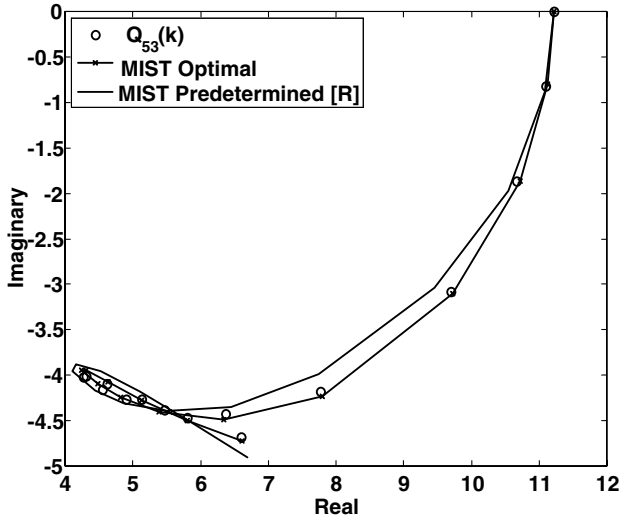

Fig. 3 Quality comparison of MIST approximation with $n_{\text{lag}} = 5$ between classical MIST results and results of complete math-programming-based fitting process.

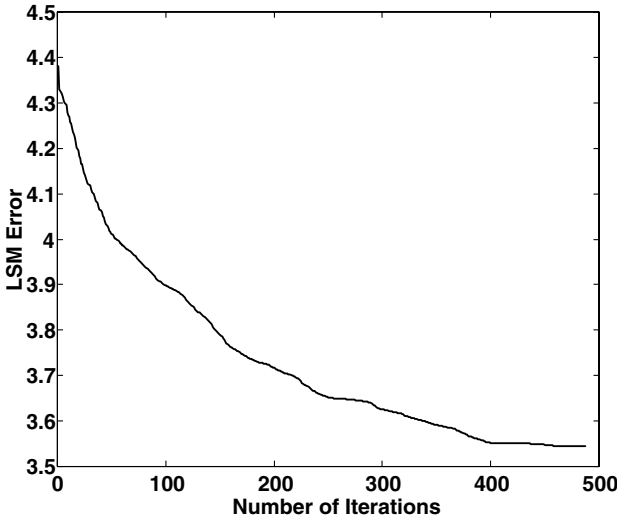

Fig. 2 Least-squares method (LSM) error during the MIST and math-programming-based fitting process.

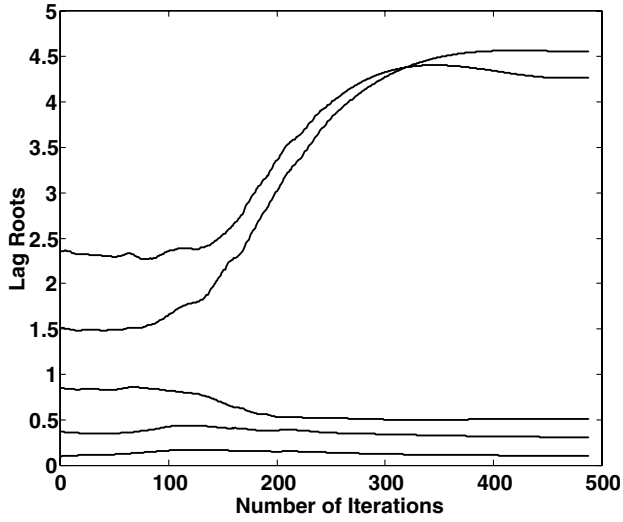

Fig. 4 Aerodynamic lag roots behavior during math-programming fitting process.

presents the behavior of the error objective during the math-programming minimization process described previously (see Sec. III), in which all elements of the MIST approximant, including the lag roots (here $n_{\text{lag}} = 5$ was chosen), were allowed to vary. One can see that the math-programming process converges after almost 500 iterations.[§] Also, as expected, the LSM error in the math-programming process is considerably smaller than one obtained by the MIST double least-squares process ($\sim$3.55 in math-programming procedure vs $\sim$4.3 in the case of MIST, see also [8]).

During the optimization, the error is reduced by more than 20% from the initial guess MIST used, increasing the quality of the match over what was achieved by the 20 iterations of conventional double least-squares process. This is clearly presented in Fig. 3 which describes the behavior of a selected Q_{53} term (at $\Lambda = 0^0$) for different reduced frequencies in both classical (double least-squares) and math-programming-based MIST cases.

In general, the lag term values are very important to the achievement of good MIST matching precision. Incorrect choice of the lag terms set can cause serious convergence problems as well as poor matching results. Some recommendations exist [19] regarding how to define the set of the lag terms with a certain distribution as a function of the number of the lag terms used n_{lag}, and the maximal value of reduced frequency $k_{\max}$.

$$\gamma_i = 1.7 k_{\max} \left(\frac{i}{n_{\text{lag}} + 1} \right)^2 \tag{33}$$

It is important to mention that in the cases studied in this work, the main difference in matching quality did not come from the convergence of the math-programming optimization process (vs not fully converged classical double least-squares MIST results). The reduction in error was mainly influenced by the fact that the lag terms were allowed to vary during the optimization. Figure 4 presents the behavior of the lag terms (with $n_{\text{lag}} = 5$) as a function of the iteration step in the math-programming optimization process. It is obvious that even though the lag terms distribution of Eq. (33) provides a good quality match based on the double least-squares process, the optimized $[R]$ matrix is very different from its origin and leads to a better match.

Figure 5 presents the sensitivity results of the elements Q_{76} and Q_{54}, based on Eq. (32) with the derivatives obtained from Eq. (31) vs the fully recalculated results for different sweep angles at the reduced frequency $k = 0.5$. The reference design for sensitivity calculation

[§]Each iteration is defined as a combination of a least-squares minimum explicit procedure ran with the new matrices $[D]$ and $[R]$, returned from the optimizer.

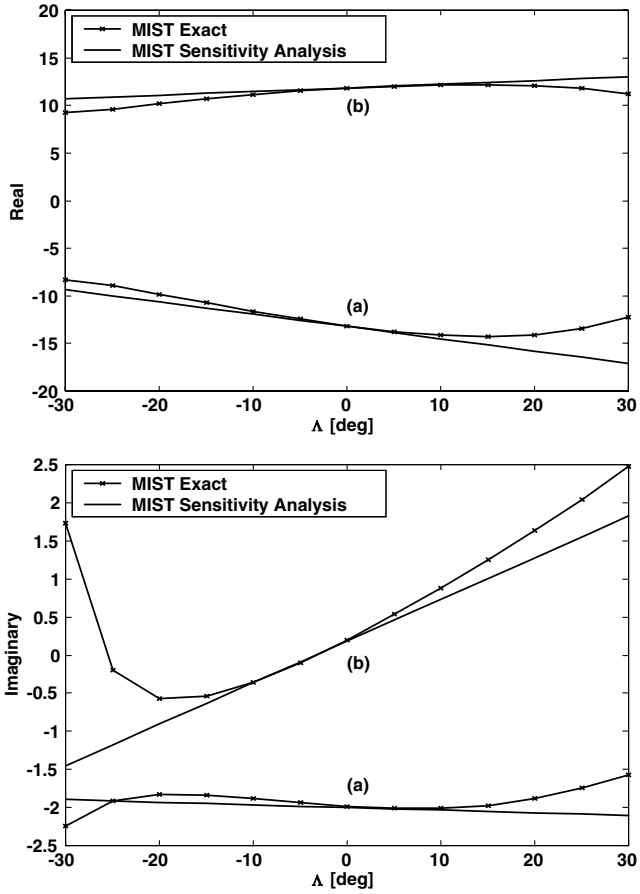

Fig. 5 Comparison between exact MIST fitting results and direct Taylor series approximation based on analysis and sensitivity results for a) Q_{54}, and b) Q_{76}.

and construction of the approximation is set at a sweep angle of 0 deg. From this representative figure, one can see that the direct Taylor series approximated results match the "exact" (fully recalculated) MIST solution well in the range of $-10^0 \leq \Lambda \leq 10^0$ as also shown in Fig. 6. The error of matching in this example does not exceed a few percents for each $[Q_{lm}(jk)]$. Further increase in the inboard sweep angle reduces the accuracy of the direct Taylor series approximation: not surprising, given the highly nonlinear dependence of unsteady aerodynamic forces on inboard wing sweep angle in the M-W wing case.

It should be noted that sensitivities of optimal solutions to problem parameter techniques are applicable to any unsteady aerodynamic functional fitting procedure based on consistent gradient-based math-programming search [2,20]. Thus, a similar technique can be applied to optimal Roger approximations where both aerodynamic poles and system matrices are determined by a gradient-based minimization process.

VI. Conclusions

A modification of the Nissim math-programming-based MIST fitting process [8,9] has been introduced and, using equations for the sensitivity of optimum solutions to problem parameters, analytic sensitivities of MIST approximants with respect to planform shape design variables have been presented. The math-programming-based fitting and its associated sensitivity analysis cover all minimum-state approximation variables, including all matrix elements and elements of the aerodynamic lag roots matrix $[R]$. The fitting technique presented displays good convergence behavior. It shows a significant influence of the lag roots distribution on the final least-squares error objective function. Behavior of MIST matrix elements as function of a planform shape variable is examined. The accuracy of the resultant shape sensitivities is verified by perfect tangency of direct Taylor series approximation curves to parametric curves representing fully calculated MIST approximants as functions of planform shape design variables. In an example of an M-W wing with variable sweep of the inner wing, the relative direct Taylor series approximation error for an approximation based on the data at a sweep angle of 0 deg does not exceed 10% in a range of $-10^0 \leq \Lambda \leq 10^0$ for the inboard sweep angle. Such an approximation, and other Taylor series approximations based on analysis and sensitivity information at a reference design point, can be used to replace exact, full analyses and allow rapid evaluation of unsteady aerodynamic and aeroelastic characteristics during multidisciplinary shape design optimization of flight vehicles.

Appendix A: Hessian Matrix for the Objective Function

$$\frac{\partial^2 f}{\partial a^{(1)}_{r_1 s_1}\partial a^{(1)}_{r_2 s_2}} = \begin{cases} 2\sum_{\nu=1}^{n_k} k_\nu^2, & r_1 = r_2, s_1 = s_2 \\ 0, & \text{else} \end{cases} \tag{A1}$$

$$\frac{\partial^2 f}{\partial a^{(1)}_{r_1 s_1}\partial a^{(2)}_{r_2 s_2}} = 0 \tag{A2}$$

$$\frac{\partial^2 f}{\partial a^{(2)}_{r_1 s_1}\partial a^{(2)}_{r_2 s_2}} = \begin{cases} 2\sum_{\nu=1}^{n_k} k_\nu^4, & r_1 = r_2, s_1 = s_2 \\ 0, & \text{else} \end{cases} \tag{A3}$$

$$\frac{\partial^2 f}{\partial a^{(1)}_{r_1 s_1}\partial d_{\bar{r}_2 p_2}} = \begin{cases} 2\sum_{\nu=1}^{n_k} \frac{k_\nu^2 \gamma_{p_2}}{k_\nu^2+\gamma_{p_2}^2} e_{p_2 s_1}, & r_1 = \bar{r}_2, \forall\ s_1, p_2 \\ 0, & \text{else} \end{cases} \tag{A4}$$

$$\frac{\partial^2 f}{\partial a^{(2)}_{r_1 s_1}\partial d_{\bar{r}_2 p_2}} = \begin{cases} -2\sum_{\nu=1}^{n_k} \frac{k_\nu^4}{k_\nu^2+\gamma_{p_2}^2} e_{p_2 s_1}, & r_1 = \bar{r}_2, \forall\ s_1, p_2 \\ 0, & \text{else} \end{cases} \tag{A5}$$

$$\frac{\partial^2 f}{\partial a^{(1)}_{r_1 s_1}\partial e_{p_2 s_2}} = \begin{cases} 2\sum_{\nu=1}^{n_k} \frac{k_\nu^2 \gamma_{p_2}}{k_\nu^2+\gamma_{p_2}^2} d_{r_1 p_2}, & s_1 = s_2, \forall\ r_1, p_2 \\ 0, & \text{else} \end{cases} \tag{A6}$$

$$\frac{\partial^2 f}{\partial a^{(2)}_{r_1 s_1}\partial e_{p_2 s_2}} = \begin{cases} -2\sum_{\nu=1}^{n_k} \frac{k_\nu^4}{k_\nu^2+\gamma_{p_2}^2} d_{r_1 p_2}, & s_1 = s_2, \forall\ r_1, p_2 \\ 0, & \text{else} \end{cases} \tag{A7}$$

$$\frac{\partial^2 f}{\partial a^{(1)}_{rs}\partial \gamma_p} = 2\sum_{\nu=1}^{n_k} k_\nu^2 \frac{k_\nu^2 - \gamma_p^2}{(k_\nu^2+\gamma_p^2)^2} d_{rp} e_{ps} \tag{A8}$$

$$\frac{\partial^2 f}{\partial a^{(2)}_{rs}\partial \gamma_p} = 4\sum_{\nu=1}^{n_k} \frac{k_\nu^4 \gamma_p}{(k_\nu^2+\gamma_p^2)^2} d_{rp} e_{ps} \tag{A9}$$

$$\frac{\partial^2 f}{\partial d_{\bar{r}_1 p_1}\partial d_{\bar{r}_2 p_2}} = \begin{cases} 2\sum_{i=1}^{n_k} \frac{k_\nu^2(k_\nu^2+\gamma_{p_1}\gamma_{p_2})}{(k_\nu^2+\gamma_{p_1}^2)(k_\nu^2+\gamma_{p_2}^2)} \sum_{m=1}^{n} e_{p_1 m} e_{p_2 m}, & \bar{r}_1 = \bar{r}_2\ \forall\ p_1, p_2 \\ 0, & \text{else} \end{cases} \tag{A10}$$

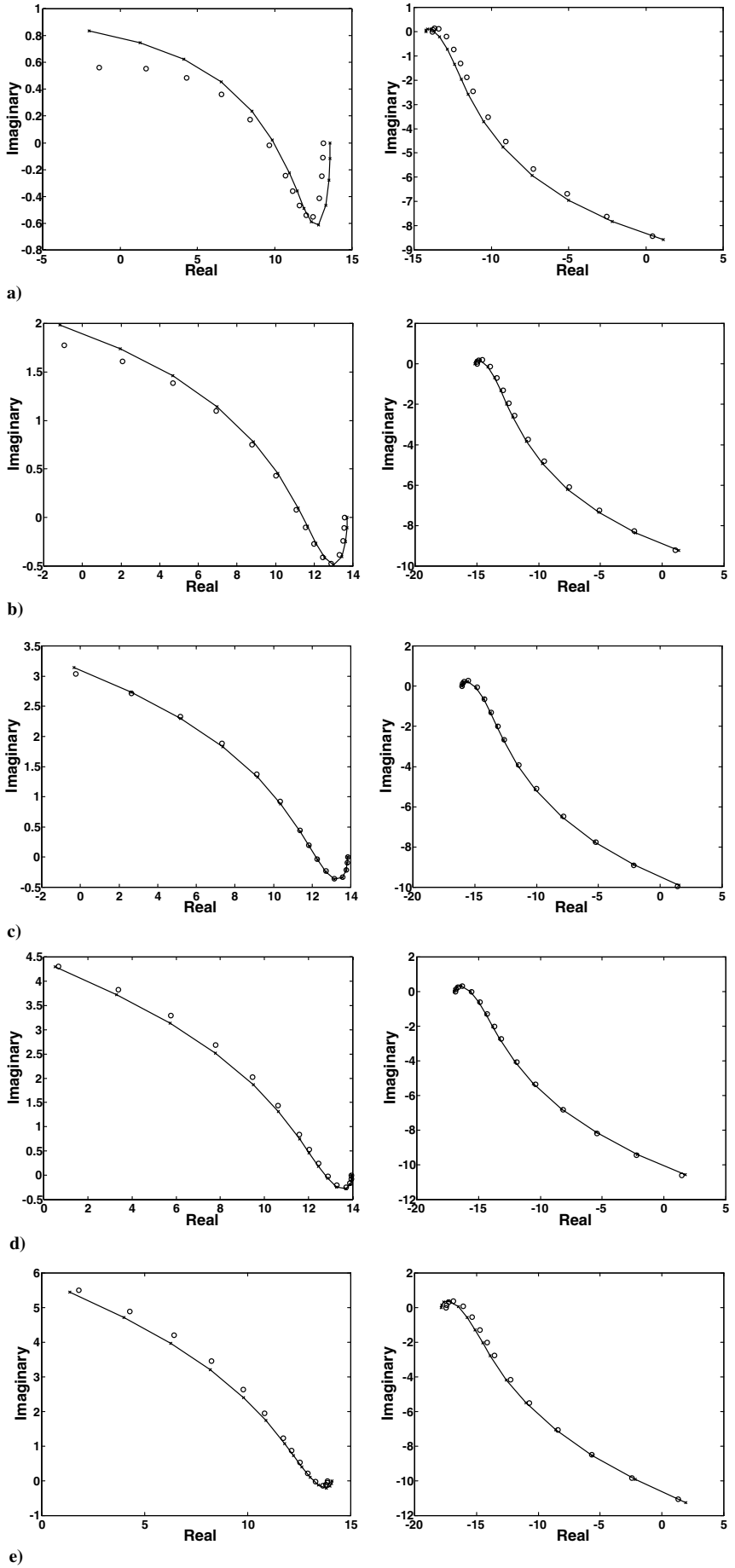

Fig. 6 Quality of MIST fitting with $n_{\text{lag}} = 5$ for Q_{76} (left) and Q_{54} (right) for a) $\Lambda = -10$, b) $\Lambda = -5$, c) $\Lambda = 0$, d) $\Lambda = 5$, and e) $\Lambda = 10$ deg.

$$\frac{\partial^2 f}{\partial d_{\bar{r}_1 p_1}\partial e_{p_2 s_2}} = 2\sum_{\nu=1}^{n_k}\frac{k_\nu^2}{(k_\nu^2+\gamma_{p_1}^2)(k_\nu^2+\gamma_{p_2}^2)}(k_\nu^2+\gamma_{p_1}\gamma_{p_2})d_{\bar{r}_1 p_2}e_{p_1 s_2} + \begin{cases} 2\sum_{\nu=1}^{n_k}\frac{k_\nu}{k_\nu^2+\gamma_{p_1}^2}[k_\nu \Delta^{\mathrm{Re}}_{\bar{r}_1 s_2}(k_\nu)+\gamma_{p_1}\Delta^{\mathrm{Im}}_{\bar{r}_1 s_2}(k_\nu)], & p_1 = p_2 \\ 0, & \text{else} \end{cases} \tag{A11}$$

$$\frac{\partial^2 f}{\partial d_{\bar{r}_1 p_1}\partial \gamma_{p_2}} = 2d_{\bar{r}_1 p_2}\sum_{\nu=1}^{n_k}\frac{k_\nu^2[-2\gamma_{p_2}k_\nu^2+\gamma_{p_1}(k_\nu^2-\gamma_{p_2}^2)]}{(k_\nu^2+\gamma_{p_1}^2)(k_\nu^2+\gamma_{p_2}^2)^2}\sum_{m=1}^{n} e_{p_1 m}e_{p_2 m} + \begin{cases} 2\sum_{\nu=1}^{n_k}\frac{k_\nu}{(k_\nu^2+\gamma_{p_1}^2)^2}\sum_{m=1}^{n}[-2k_\nu\gamma_{p_1}\Delta^{\mathrm{Re}}_{\bar{r}_1 m}(k_\nu)+(k_\nu^2-\gamma_{p_1}^2)\Delta^{\mathrm{Im}}_{\bar{r}_1 m}(k_\nu)]e_{p_1 m}, & p_1 = p_2 \\ 0, & \text{else} \end{cases} \tag{A12}$$

$$\frac{\partial^2 f}{\partial e_{p_1 s_1}\partial e_{p_2 s_2}} = \begin{cases} 2\sum_{\nu=1}^{n_k}\frac{k_\nu^2(k_\nu^2+\gamma_{p_1}\gamma_{p_2})}{(k_\nu^2+\gamma_{p_1}^2)(k_\nu^2+\gamma_{p_2}^2)}\sum_{l=1}^{n} d_{l p_2}d_{l p_1}, & s_1 = s_2 \\ 0, & \text{else} \end{cases} \tag{A13}$$

$$\frac{\partial^2 f}{\partial e_{p_1 s_1}\partial \gamma_{p_2}} = 2e_{p_2 s_1}\sum_{\nu=1}^{n_k}\frac{k_\nu^2[-2\gamma_{p_2}k_\nu^2+\gamma_{p_1}(k_\nu^2-\gamma_{p_2}^2)]}{(k_\nu^2+\gamma_{p_1}^2)(k_\nu^2+\gamma_{p_2}^2)^2}\sum_{l=1}^{n} d_{l p_1}d_{l p_2} + \begin{cases} 2\sum_{\nu=1}^{n_k}\frac{k_\nu}{(k_\nu^2+\gamma_{p_1}^2)^2}\sum_{l=1}^{n}[-2k_\nu\gamma_{p_1}\Delta^{\mathrm{Re}}_{l s_1}(k_\nu)+(k_\nu^2-\gamma_{p_1}^2)\Delta^{\mathrm{Im}}_{l s_1}(k_\nu)]d_{l p_1}, & p_1 = p_2 \\ 0, & \text{else} \end{cases} \tag{A14}$$

$$\frac{\partial^2 f}{\partial \gamma_{p_1}\partial \gamma_{p_2}} = 2\sum_{\nu=1}^{n_k}\frac{k_\nu^2[4k_\nu^2\gamma_{p_1}\gamma_{p_2}+(k_\nu^2-\gamma_{p_1}^2)(k_\nu^2-\gamma_{p_2}^2)]}{(k_\nu^2+\gamma_{p_1}^2)^2(k_\nu^2+\gamma_{p_2}^2)^2}\sum_{l=1}^{n} d_{l p_1}d_{l p_2}\sum_{m=1}^{n} e_{p_1 m}e_{p_2 m} + \begin{cases} -4\sum_{\nu=1}^{n_k}\frac{k_\nu}{(k_\nu^2+\gamma_{p_1}^2)^3}\sum_{l=1}^{n}\sum_{m=1}^{n}[k_\nu(k_\nu^2-3\gamma_{p_1}^2)\Delta^{\mathrm{Re}}_{lm}(k_\nu)+\gamma_{p_1}(3k_\nu^2-\gamma_{p_1}^2)\Delta^{\mathrm{Im}}_{lm}(k_\nu)]d_{l p_1}e_{p_1 m}, & p_1 = p_2 \\ 0, & \text{else} \end{cases} \tag{A15}$$

Appendix B: Shape Derivative of Objective Functions Gradient

$$\frac{\partial^2 f}{\partial DV\partial a_{rs}^{(1)}} = 2\sum_{\nu=1}^{n_k} k_\nu \frac{\partial \Theta^{\mathrm{Im}}_{rs}(k_\nu)}{\partial DV} \tag{B1}$$

$$\frac{\partial^2 f}{\partial DV\partial a_{rs}^{(2)}} = -2\sum_{\nu=1}^{n_k} k_\nu^2 \frac{\partial \Theta^{\mathrm{Re}}_{rs}(k_\nu)}{\partial DV} \tag{B2}$$

$$\frac{\partial^2 f}{\partial DV\partial d_{\bar{r}p}} = 2\sum_{\nu=1}^{n_k}\frac{k_\nu}{k_\nu^2+\gamma_p^2}\sum_{m=1}^{n}\left(k_\nu\frac{\partial \Theta^{\mathrm{Re}}_{\bar{r}m}(k_\nu)}{\partial DV}+\gamma_p\frac{\partial \Theta^{\mathrm{Im}}_{\bar{r}m}(k_\nu)}{\partial DV}\right)e_{pm} \tag{B3}$$

$$\frac{\partial^2 f}{\partial DV\partial e_{ps}} = 2\sum_{\nu=1}^{n_k}\frac{k_\nu}{k_\nu^2+\gamma_p^2}\sum_{l=1}^{n}\left(k_\nu\frac{\partial \Theta^{\mathrm{Re}}_{ls}(k_\nu)}{\partial DV}+\gamma_p\frac{\partial \Theta^{\mathrm{Im}}_{ls}(k_\nu)}{\partial DV}\right)d_{lp} \tag{B4}$$

$$\frac{\partial^2 f}{\partial DV\partial \gamma_p} = 2\sum_{\nu=1}^{n_k}\frac{k_\nu}{(k_\nu^2+\gamma_p^2)^2}\sum_{l=1}^{n}\sum_{m=1}^{n} \times\left(-2k_\nu\gamma_p\frac{\partial \Theta^{\mathrm{Re}}_{lm}(k_\nu)}{\partial DV}+(k_\nu^2-\gamma_p^2)\frac{\partial \Theta^{\mathrm{Im}}_{lm}(k_\nu)}{\partial DV}\right)d_{lp}e_{pm} \tag{B5}$$

where

$$\frac{\partial \Theta^{\mathrm{Re}}_{lm}(k)}{\partial DV} = -\frac{\partial\,\mathrm{Re}[q_{lm}(jk)-q_{lm}(0)]}{\partial DV} \tag{B6}$$

and

$$\frac{\partial \Theta^{\mathrm{Im}}_{lm}(k)}{\partial DV} = -\frac{\partial\,\mathrm{Im}[q_{lm}(jk)]}{\partial DV} \tag{B7}$$

Acknowledgment

Support by NASA Langley Research Center (Peter Coen, grant monitor) is gratefully acknowledged.

References

[1] Karpel, M., "Design for Active Flutter Suppression and Gust Alleviation Using State Space Aeroelastic Modeling," *Journal of Aircraft*, Vol. 19, No. 3, March 1982, pp. 221–227.

[2] Tiffany, S. H., and Adams, W. M., "Nonlinear Programming Extensions to Rational Function Approximations of Unsteady

Aerodynamic Forces," NASA TP 2776, 1988; also AIAA Paper 87-0854.
[3] Karpel, M., "Time-Domain Aeroservoelastic Modeling Using Weighted Unsteady Aerodynamic Forces," *Journal of Guidance, Control, and Dynamics*, Vol. 13, Jan. 1990, pp. 30–37.
[4] Karpel, M., and Strul, E., "Minimum-State Unsteady Aerodynamic Approximations with Flexible Constraints," *Journal of Aircraft*, Vol. 33, No. 6, 1996, pp. 1190–1196.
[5] Karpel, M., "Reduced-Order Models for Integrated Aeroservoelastic Optimization," *Journal of Aircraft*, Vol. 36, No. 1, Jan.–Feb. 1999, pp. 146–155.
[6] Mor, M., and Livne, E., "Minimum State Unsteady Aerodynamics for Aeroservoelastic Configuration Shape Optimization of Flight Vehicles," *AIAA Journal*, Vol. 43, No. 11, Nov. 2005, pp. 2299–2308.
[7] Mor, M., and Livne, E., "Sensitivities and Approximations for Aeroservoelastic Shape Optimization with Gust Response Constraints," *Journal of Aircraft*, Vol. 43, No. 5, Sept.–Oct. 2006, pp. 1516–1527.
[8] Nissim, E., "Formulation of the Minimum-State Approximation as a Non-Linear Optimization Problem," *Journal of Aircraft*, Vol. 43, No. 4, July–Aug. 2006, pp. 1007–1013.
[9] Nissim, E.," Uniqueness of the Minimum State Representation," *Journal of Aircraft*, Vol. 42, No. 5, Sept.–Oct. 2005, pp. 1339–1340.
[10] Haftka, R. T., and Gurdal, Z., *Elements of Structural Optimization*, 3rd ed., Kluwer Academic, Norwell, MA, 1992.
[11] Yates, E. C., Jr., "Aerodynamic Sensitivities from Subsonic, Sonic, and Supersonic Unsteady, Nonplanar Lifting Surface Theory," NASA TM 100502, Sept. 1987.
[12] Yates, E. C., Jr., "Integral Equation Methods in Steady and Unsteady Subsonic, Transonic, and Supersonic Aerodynamics for Interdisciplinary Design," NASA TM 102677, May 1990.
[13] Livne, E., and Li, W.-L., "Aeroservoelastic Poles: Their Analytic Sensitivity and Alternative Approximations in Wing Planform Shape Synthesis," AD-Vol. 44, *Aeroelasticity and Fluid Structure Interaction Problems*, edited by P. P. Friedmann and, J. C. I. Chang, American Society of Mechanical Engineers, New York, 1995, pp. 99–123.
[14] Livne, E., and Li, W-L., "Aeroservoelastic Aspects of Wing/Control Surface Planform Shape Optimization," *AIAA Journal*, Vol. 33, No. 2, Feb. 1995, pp. 302–311.
[15] Li, W-L., and Livne, E., "Analytic Sensitivities and Approximations in Supersonic and Subsonic Wing/Control Surface Unsteady Aerodynamics," *Journal of Aircraft*, Vol. 34, No. 3, May–June 1997, pp. 370–379.
[16] Livne, E., "Integrated Aeroservoelastic Optimization: Status and Progress," *Journal of Aircraft*, Vol. 36, No. 1, Jan.–Feb. 1999, pp. 122–145.
[17] Koo, K. N., "Aeroelastic Characteristics of Double-Swept Isotropic and Composite Wings," *Journal of Aircraft*, Vol. 38, No. 2, March–April 2001, pp. 343–348.
[18] Schaeffer, H. G., *MSC. NASTRAN Primer for Linear Analysis*, 2nd ed., MSC Software, Santa Ana, CA, 2001.
[19] Anon., *ZAERO: An Engineers' Toolkit for Aeroelastic Solutions*, ZONA Technology, Scottsdale, AZ, 2004.
[20] Eversman, W., and Tewari, A., "Consistent Rational-Function Approximation for Unsteady Aerodynamics," *Journal of Aircraft*, Vol. 28, No. 9, Nov. 1991, pp. 545–552.

N. Alexandrov
Associate Editor